First ECRH Experiments in ASDEX-Upgrade

F. Leuterer, H. Brinkschulte, F. Monaco, M. Münich, A.G. Peeters,
G. Pereverzev, F. Ryter, W. Suttrop, ASDEX-Upgrade group,
Max Planck Institut für Plasmaphysik, 85740 Garching, Germany

G. Gantenbein, W. Kasparek, ECRH group, *Inst. f. Plasmaforschung Stuttgart*;
ECRH Group, *Inst. Appl. Physics, Nizhny Novgorod*;

Abstract

The variation of the global confinement time is found to depend on the radius of localized ECRH power deposition. Measurements of the risetime of electron temperature from ECE give broader profiles as the calculated ECRH deposition profiles. This is explained by diffusion within the time interval which is necessary for the measurement. Experiments with modulated ECRH for heat pulse propagation studies are described in a separate paper /1/.

1. The ECRH system

At ASDEX-Upgrade we are presently installing an ECRH system with a total power of 2 MW (resp. 2.8 MW) for a pulse length of 2 sec (resp. 1 sec), generated by 4 gyrotrons. The system is expected to be ready in spring 1997. The frequency is 140 GHz, the working mode is the second harmonic x-mode.

Two gyrotrons at a time are fed from one common power supply via one series modulator tube. This modulator is used for switching on and off the high voltage both for modulation (up to 1 kHz) and for safety reasons. Faster power modulation with a frequency up to 30 kHz is possible when the high voltage is reduced only by about 30%, which is sufficient to stop the oscillation in the gyrotron, but maintains the beam current.

The power is transmitted via four transmission lines partly quasioptical, and partly via a HE-11 waveguides /2/. The quasioptical part consists of beam correcting mirrors, polarization mirrors, elliptical and plane mirrors, and a mirror directional coupler within the beam matching box right after the gyrotron output. The waveguide part includes a mode coupling section to provide the necessary broad power density profile for transmission through the boron nitride torus window, and a mitre bend directional coupler just before the torus input. Both directional couplers give a clear signal free of interferences which can be calibrated for measuring the transmitted power. The launching is at the midplane from the low field side. Steerable mirrors (graphite with copper and gold coating) allow to vary the direction of the beam both poloidally (± 35°) and toroidally (± 25°) as necessary for localized on or off axis power deposition and current drive. The beam is focused such that without plasma the beam waist with $w_0 = 21.2$ mm is located at half minor radius on the high field side.

In a first step we started experiments using another 140 GHz gyrotron with 0.5 MW / 0.5 sec of which 0.4 MW arrive at the torus input. The losses are due to power contained in higher order modes of the gyrotron output (estimated to 15%), which is not transmitted, and to ohmic losses in the mirrors and mitre bends (estimated to 7%). The adjustment of the mirror transmission line is without problems. However, the coupling of the quasioptical beam to the HE-11 mode in the waveguide turned out to be very sensitive to the quality of the Gaussian beam. Slight imperfections, like a rest of astigmatism, leads to excitation of additional waveguide modes, which, although containing only a small fraction of the power, can modify the power flow in the waveguides due to interferences and thus also the power density profile at the waveguide output and in the torus window. Improvement requires an accurate knowledge of the beam parameters.

2. ECRH heating in an ohmic plasma

Application of ECRH into ohmically heated plasmas leads to electron heating, and as a consequence to a drop in the loop voltage. However, this depends on the location of power deposition. In figs.1a and 1b we compare two shots where the power deposition was inside (r_{pol}<0.38), respectively outside (r_{pol}≈0.77), of the sawtooth inversion radius (r_{pol}≈0.4).

In the first case the loop voltage U_{loop} decreases very slowly, and at the end of the 0.5 sec pulse, the global confinement time τ_E, determined from the energy content W_{mhd} divided by the total power P_{tot}, reaches the same value as during the preceding ohmic phase. Thus τ_E seems not to be degraded with the increased total power input.

In the second case the loop voltage decreases faster, and the global confinement time at the end of the pulse reaches a constant value which is less than that in the ohmic phase, scaling as $\tau_{E,oh}/\tau_{E,ecrh} \approx (P_{tot}/P_{oh})^{-0.5}$, i.e. it shows the usual confinement degradation with power. The electron temperature increase in the central region (≈ 70 eV) is in this case less than in the first case (≈ 300 ev). The internal inductance and the sawtooth frequency remain constant, whereas they increase in the case of the central power deposition (l_i = 1.22 to 1.26). Such an increase of l_i indicates better confinement /3/.

We conclude that the influence of additional electron heating on confinement depends also on the localization of the power depositon.

3. Power deposition profile

The system is designed to achieve very localized power deposition. Calculations including diffraction effects /4/ show that we should get different power deposition profiles in the two cases of off axis heating as shown in fig. 2. In the case where the resonance magnetic field is off axis and the rf-beam arrives there perpendicular to the flux surface, the deposition profile is determined by the imaginary part of the wavevector. This leads to a very narrow profile with a full half width of ≈ 8 mm. On the other hand, if the ray is about tangent to the flux surface at the resonance, the deposition profile is determined mainly by the beam cross section, leading to a profile with full half width of ≈ 30 mm. In order to get an estimate of the experimental power deposition profile, we determine the rate of change of the electron temperature dT_e/dt at the switch on of the rf-power. Fig. 3 shows examples of ECE signals from different radii. The rise of T_e occurs instantaneously with the switch on, or delayed, depending on the radial position. In figs. 4 and 5 we plot dT_e/dt at the time where we observe an increase of T_e together with the delay Δt. We consider only those data points without measurable delay to represent a maximum estimated width of the deposition profile (dotted line). These profiles are, however, wider than the ones calculated for these particular shots, which are also shown in the figures as dashed lines. The difference in radial position between calculated and measured maximum may be due to calibration errors, and is not further discussed here. The measurements were taken at the low field side of the torus, while the power was deposited at the high field side (fig. 4) or in the upper part of the plasma (fig. 5) as shown in fig. 2.

The broader dT_e/dt-profiles can be understood by considering the one dimensional linearized heat diffusion equation. Assuming a Gaussian power deposition profile $\exp(-x^2/x_o^2)$, a step function for the time dependence and a constant electron heat diffusivity χ, we can calculate the temperature response as /5/:

$$\tilde{T}(x,t) = \text{const. } A \int_{(1+t/A)^{-1/2}}^{1} \exp(-(x/x_0)^2\zeta^2)/\zeta^2 d\zeta \qquad \text{equ.(1)}$$

Here the quantity $A = x_o^2/(4\chi)$ represents a characteristic time for diffusion. Numerical evaluation of equ.(1) shows that the heated zone widens by a factor of 2 within 10 characteristic times. Taking for χ a value of 1 m^2/sec, we obtain A = 4 µsec in the case x_0 = 4 mm, and A = 56 µsec for x_0 = 15 mm. In ASDEX Upgrade it takes about 1 µsec for a 1 kV electron to run once around the torus. For deposition at r/a≈0.5 the poloidal circumference of the flux surface is ≈2.5 m and with a rf-beam diameter of 50 mm it takes about 50 µsec to heat all the flux surface. Furthermore, to determine dT_e/dt with sufficient reliability we need ≈500 µsec >> A. During this time considerable diffusion has occured. For the narrow profile in fig. 4 this corresponds to ≈120 A which leads, evaluating equ.(1), to a broadening by a factor of ≈5.5, and thus comes close to the measured width. Similarly, for the broader profile of fig. 5 the full flux surface is heated within one characteristic time, and the time for measurement corresponds to ≈10 A. In this case diffusion widens the heated zone to about two times the power deposition width, again similar to what we measure.

We conclude that the dT_e/dt-profiles cannot be simply taken as the power deposition profiles calculated from the wave absorption. Diffusion during the time which is necessary for the measurement of dT_e/dt must be taken into account.

References

/1/ Ryter F., this conference, paper OP3

/2/ Förster W., Proc. 9th. Workshop on ECE and ECRH, Borrego Springs, California, 1995, p. 565-573

/3/ Hoang G.T. et al., 19th EPS Conference on Controlled Fusion and Plasma Physics, Innsbruck 1992, Europhysics Conference Abstracts Vol. 16C, part 1, p.27

/4/ Peeters A.G., this conference

/5/ Tychonoff A.N., Samarski A.A., „Differetial Equations in mathematical Physics", VEB Dtsch. Verlag d. Wissenschaften, Berlin 1959

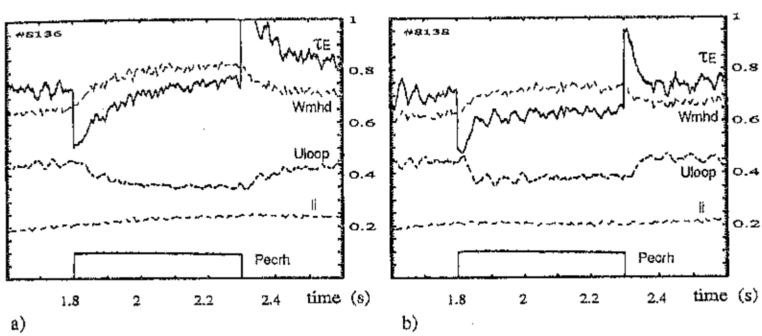

Fig. 1 Time traces of Pecrh, Uloop, Wmhd, li, τE for power deposition a) inside and b) far outside of the sawtooth inversion radius. Ip = 1 MA, ne = 4 10^19 m^-3, Bt = 2.5 T

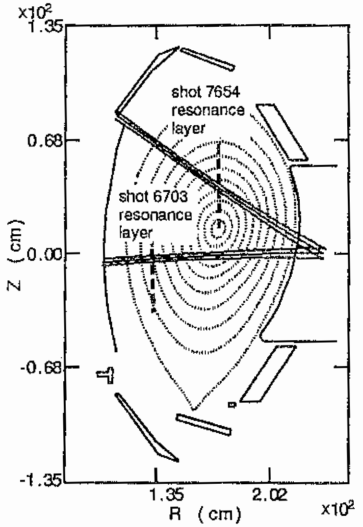

Fig. 2. Ray projections in the poloidal cross section for two cases of off-axis power deposition.

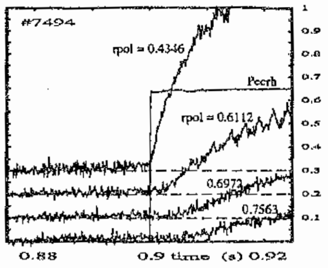

Fig.3 ECE time traces at different radii

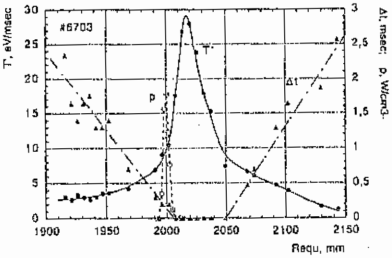

Fig.4 Calculated deposition profile p (dashed line), measured rate of temperature increase T' and measured delay time Δt; Bt = -2 T, phi = 0°

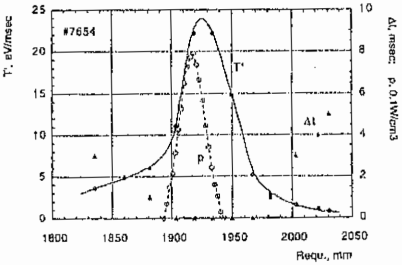

Fig.5 Calculated deposition profile p (dashed line), measured rate of temperature increase T', and measured delay time Δt; Bt = -2.5 T, phi = 30°